Pitchaimuthu Pathalamuthu[1],
Shamsheer Thameem Shahana[2],
Uthayakumaran Nivedha[2],
Arjunan Siddharthan[3*],
Venkateshwarapuram
Rengaswami Giridev[2*]

Analysis of the Inhomogeneity of an Electrospun Mat Produced Using Static and Dynamic Collectors of Different Template Design, Including its Mitigation

[1] Department of Chemical Engineering,
Anna University,
Chennai-600025, India

[2] Department of Textile Technology,
Anna University,
Chennai-600025, India
* E-mail:vrgiridev@annauniv.edu

[3] Department of Production Technology,
Anna University,
Chennai-600044, India
* E-mail:sidharth@annauniv.edu

Abstract

In an electrospinning process, as the deposition of fibres occurs randomly over the collector, the mats produced are generally expected to have homogeneous properties throughout the mat. This study compares the ultimate tensile strength, porosity, thickness and morphology of the different portions of mats sectioned at various angular locations. The influence of the template design and mode of operation of the collectors on the properties of electrospun mats were investigated. The inhomogeneity in the properties of the electrospun mat produced using stationary collectors was significant, irrespective of the different template design of the collectors. However, the collectors operated in the dynamic mode decrease variations in the properties among the different sections of the electrospun mats. By choosing a particular template design and mode of operation of the collector, an electrospun mat of desired orientation can be achieved.

Key words: *electrospinning, template, collectors, alignment, pore, mechanical property.*

Introduction

Electrospinning is a cost effective and versatile technique that employs electrostatic forces to produce polymer fibres of a diameter in the range of a few microns to tens of nanometers. The major components of a typical electrospinning setup are the spinneret, fibre collector, and high voltage power system. As the electrospinning process is capable of producing mats with the physical and chemical properties desired, it finds application in the various fields like scaffolds for tissue engineering, sensors, membranes, catalysts, anti-counterfeiting, water proof fabric and solar cells [1, 2].

Due to the bending instability of the charged liquid jets, the electrospun fibres

are generally deposited as a nonwoven mat with a random assembly of fibres over the collector surface. The preparation of well-aligned fibres with a patterned structure is desired for certain biomedical applications, fibre reinforced composites as well as microelectronic and photonic devices [3-9]. Electrospun mats with an ordered cellular organisation of fibres and template structure have potential application for functional tissue or organ regeneration [10-11]. Radially aligned fibres are more suitable for biomedical applications [12]. Collectors with defined patterns are used to develop modern air filters [13]. Various approaches like the application of electric potential and use of a collector plate with template are reported to tailor the architecture and pattern desired. The use of a rotating collector plate with grids produced an electrospun mat with 76% fibre alignment. In the case of the dynamic mode of operation of the collector plate, the fibres are dragged by the force generated by the rotation of the collector. The magnitude of the drag force is higher for continuous collectors like discs and drums than that of collectors with holes [14].

There is limited literature, to our knowledge, on the analysis of the variation in properties among the different sections of electrospun mats collected over a collector plate, which may be a concern from an application point of view. The distribution of the nanofiber diameter and quality of a nanofiber web were

analysed [15]. The objective of the present work was to investigate the influence of the template design and the mode of operation of the collector plate on the inhomogeneity in the properties of samples sectioned at different angles from the circular electrospun mat.

## Materials and methods

Materials

To evaluate the influence of the template design and dynamic mode of operation of the collector on the properties of an electrospun mat, polyacrylonitrile (PAN) was selected as the material for study. The solution for electrospinning was produced by dissolving PAN in N, N dimethyl formamide (DMF, Molecular Weight 73.10, SRL, India) in a proportion of 12% (wt./vol.) under constant magnetic stirring at room temperature.

Preparation of the electrospun mat

Electrospinning was carried out by using a laboratory setup consisting of an infusion pump, high voltage source and collector assembly. Based on the initial trials, a voltage of 13 kV and distance of 150 mm between the needle and collector surface were selected. Electrospun mats were prepared with the use of collectors of different template design both in the static and dynamic mode of operation. The collector during the dynamic mode of operation was rotated at 300 rpm with the use of a motor and regulated power supply. The electrospun mat was collect-
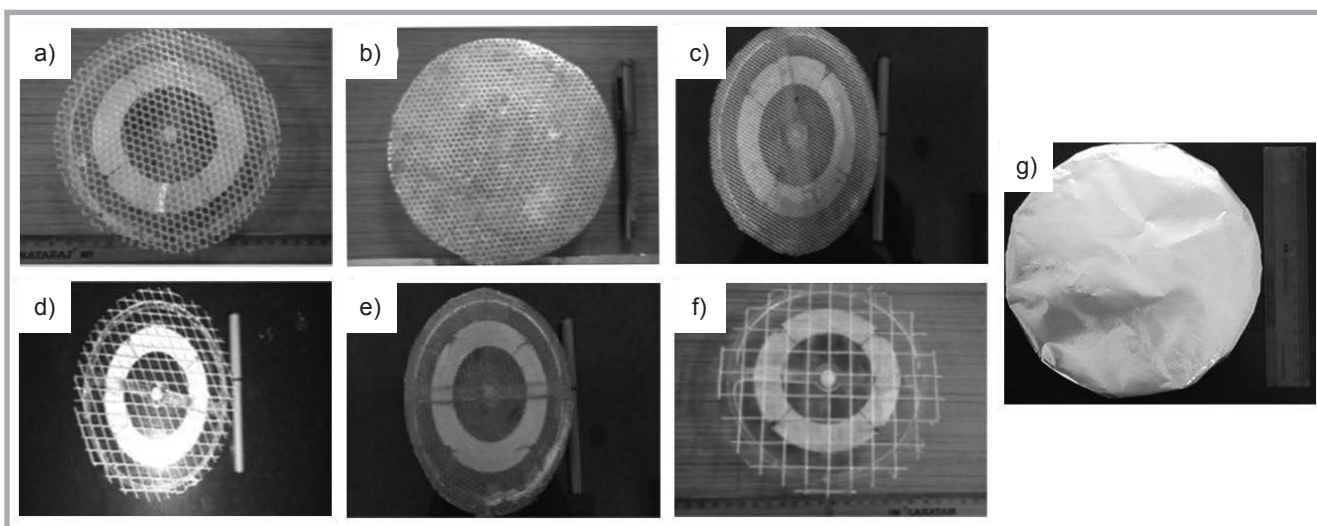
Figure 1. *Collectors of different templates used for collecting electrospun mats: a) hexagonal shaped grid (H), b) circular shaped pattern (C), c) rhombus shaped grid – small (RS), d) rhombus shaped grid – large (RL), e) square shaped grid – small (SS), f) square shaped grid – larger (SL), and g) plain collector-aluminium foil (PC).*
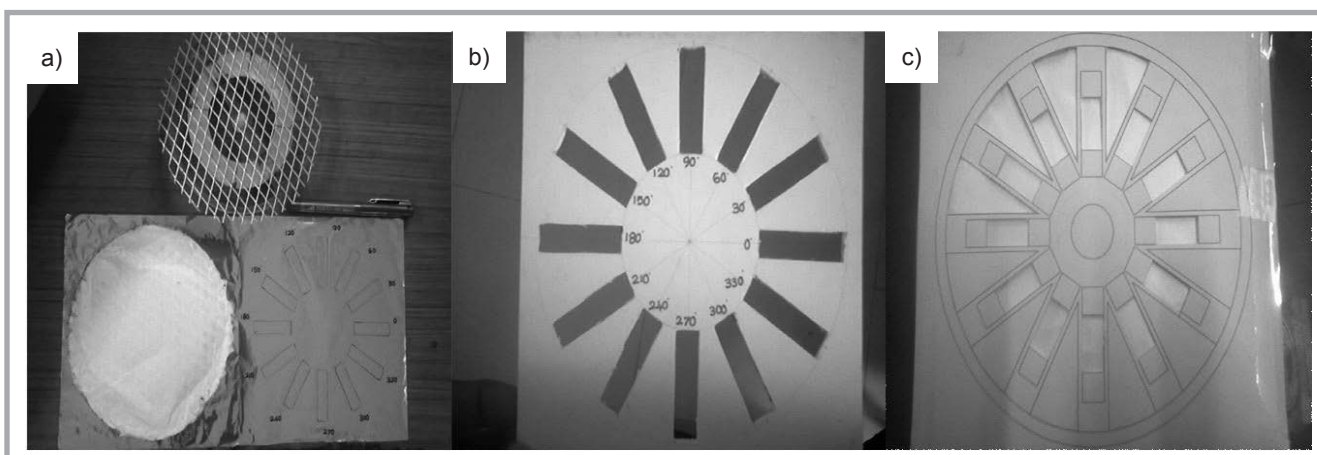
Figure 2. *Electrospun mat and sample preparation for tensile testing: a) electrospun mat wrapped with aluminium foil, b) stencil made of chart paper for sectioning the elctrospun mat, c) tensile test sample covered with chart paper at the gripping portion.*

ed for a time period of 4 h for both the static and dynamic mode of operation of the collectors. The solution was discharged at a constant rate of 1 ml/h with the use of a syringe pump by maintaining the room temperature at 26 °C. The seven different template designs of aluminium collector plate used for the collection of electrospun mats are shown in **Figure 1**. The dimensions of the hole, thickness, surface area and porosity of the collector plate are listed in **Table 1**.

Microscopic analysis

The morphology of the mat was characterised by a Scanning Electron Microscope (SEM) (HITACHI-S3400N, Hitachi High Technologies Corporation, Tokyo, Japan) in five different places. From the SEM images, the fibre diameter and number of binding points were meas-

ured using DIGIMIZER, image analysis software.

Mechanical testing

The thickness of the electrospun mat prepared using different collectors was measured by using a micrometer. The thickness of the electrospun mat was measured at different points within different angular sections. The mechanical properties of the electrospun mat, namely the ultimate tensile stress and Young's modulus, were evaluated using a Universal Testing Machine (UTM, INSTRON 3369, USA). With the help of a surgical knife, the mat was carefully removed from the collector and specimens of 20 mm ×10 mm dimensions as per ASTM D88 were sectioned from the electrospun mat at different angles (0°, 30°, 60°, 90°...330°), as shown in *Fig-*

ure 2.b. The cross speed for the tensile test was 5 mm/min.

An in-house developed method for indicating the flexural strength of the electrospun mat through measurement of the deflection in response to a static load was done using the setup shown in *Figure 3*. The electrospun mat was fixed to polypropylene (PP) supports with adhesive tape. A plastic ball of 2.2 g weight was placed above the mat. The mat was roughly triangular in shape, which was the portion left after sectioning samples for tensile testing, as shown in *Figure 2.b*. The deflection of the mat due to the weight of the ball was measured using a vernier calliper.

Determination of pore size

The pore size distribution of the electrospun mat was determined using a capil-

lary flow porometer (Porous Materials Inc., USA). A wetting liquid, Galwick™ (Porous Materials Inc., USA) was applied to fill the pores in the electrospun mat at differential pressures of nitrogen. The supply of gas was slowly increased to the sample so as to remove the liquid filling the pores and entrain gas flow. The differential pressure and flow rates through dry and wet electrospun mats were used for determination of pore size. The relationship between the pore size and corresponding pressure is given by the Young Laplace *Equation (1)*:

$$R = \frac{2\gamma}{\Delta P}cos\Theta \qquad (1)$$

where R, ΔP, γ and Θ represents the radius of the pore, ΔP – differential gas pressure, the surface tension of the wetting liquid (Galwick™, $\gamma = 15.9\times10^{-5}$N/cm) and wetting angle, respectively.

Analysis of fibre orientation using 2D fast fourier transform (FFT) of SEM images

Quantitative analysis of an SEM image to evaluate fibre orientation was carried out using an image processing tool – 2D FFT transformation. The 2D FFT function converts the spatial information of an image into a mathematically defined frequency domain. This frequency domain maps the rate at which the pixel intensities change in the spatial domain.

All the SEM images were analysed in the 'uncompressed .tif' file format to preserve image integrity. The grayscale 8-bit image was cropped to 2048×2048 pixels for analysis. ImageJ software (NIH, http://rsb.info.nih.gov/ij) was supported by an oval profile plug-in (authored by William O' Connnell) and was used to conduct 2D FFT analysis. Using Adobe® photoshop, SEM images of the electrospun mat were transformed to 2048 x 2048 pixel, feathered to 20 px, converted to the 8 bit gray scale and flattened. The amended images were then processed for 2D FFT in ImageJ and radial summation was measured through the oval plugin in ImageJ tool.

The FFT output image displays gray scale pixels and their distribution pattern, reflecting that a degree of fiber alignment was present in the original SEM image. The pixel intensities were summed along each radius and plotted as a function of the angle of acquisition. The degree of alignment presented in the original SEM image was reflected by the height and overall shape of the peak present in the
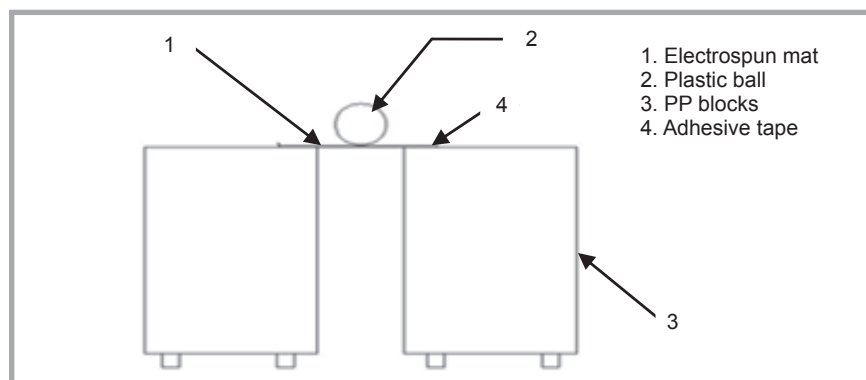

Figure 3. Test setup for evaluating the deflection of the electrospun mat for a static load.

1. Electrospun mat
2. Plastic ball
3. PP blocks
4. Adhesive tape

plot with the angle in x-axis and gray scale in the y-axis. The altitude of the peak in the graph described the intensity of fiber at a particular angle [16].
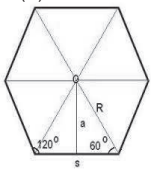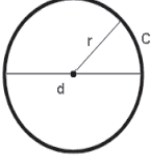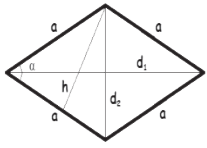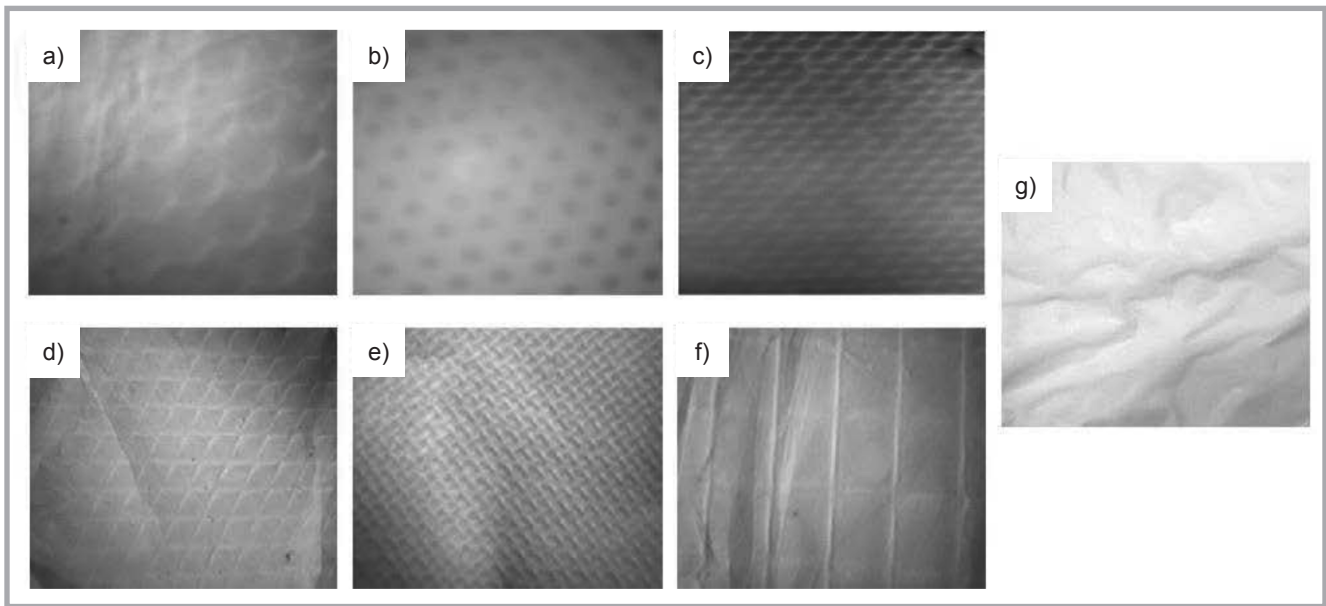
Result and discussion

Morphological features of electrospun mats

Photographs of the electrospun mat produced using stationary collectors of different template design are shown in *Figure 4*. All the images show a reproduction of the design of the template of the collector in the electrospun mat. SEM images of the electrospun mat at 7.5 K magnification revealed the network structure and diameter of nanofibres constituting the nonwoven mat. A distinct variation in the network structure and alignment of nanofibres were observed among the electrospun

Table 1. Features of templates of different collectors made of aluminium.

S. No.	Grid shapes	Thickness, mm	Surface area, m²	Porosity of collector, %
1	Hexagon (H) of side: a = 2.5 mm	1	0.008	53
2	Circle (C) of radius: r = 1 mm	0.5	0.012	42
3	Rhombus small (RS) d1 = 3 mm; d2 = 2 mm	1	0.013	28
4	Rhombus large (RL) d1 = 15 mm; d2 = 10 mm	1	0.003	84
5	Square-small (SS) of side:1.5 mm	1	0.007	58
6	Square-large (SL) of side:15 mm	1	0.002	89
7	Plain collector (PC)	0.05	0.018	0

Figure 4. *Photographic image of electrospun mat produced using a collector of different template design: a) H, b) C, c) RS, d) RL, e) SS, f) SL, g) PC.*
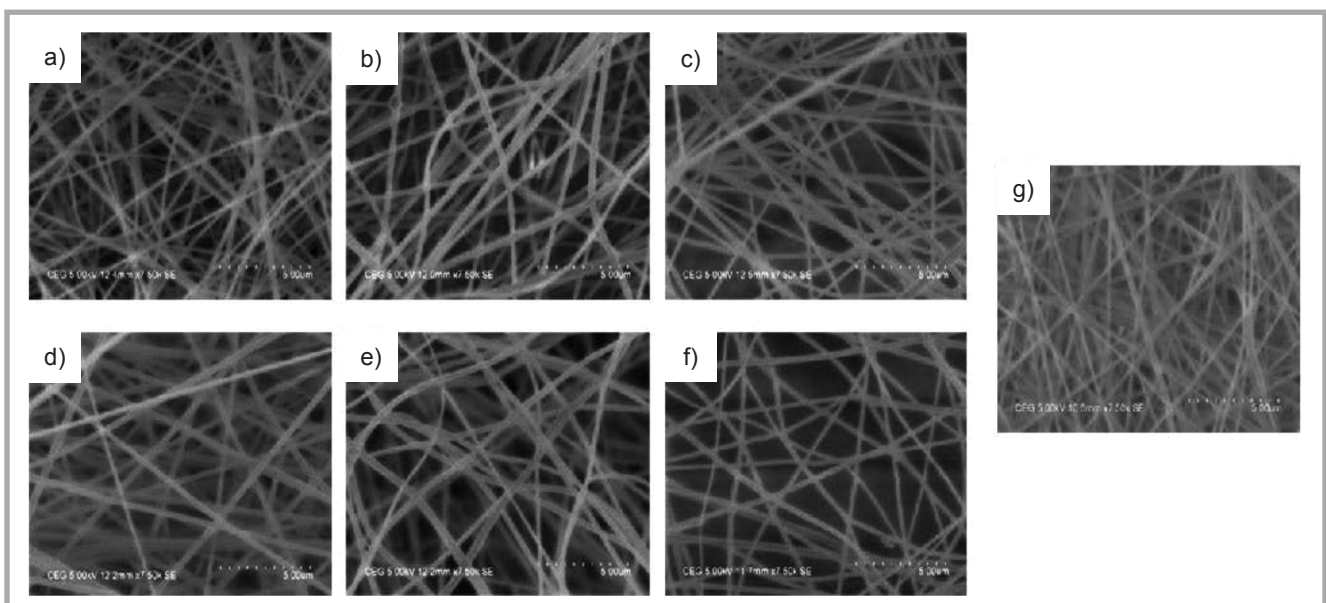
mats produced using collectors of different template design *(Figure 5* and *6)*. SEM images of the electrospun mat produced using a static and rotating collector of a specific template design, showed a notable change in the alignment of fibres.

The average diameter of the electrospun fibres are listed in *Table 2*. The diameters of fibres of electrospun mats produced using stationary collectors range from 165 to 286 nm, whereas the dynamic mode of operation of collectors produced fibres with a diameter in the range of 109 to 426 nm. However, fibres of the lowest diameter were observed in the electrospun mat that was produced by using collector plate (SS) operated in the dynamic mode.

The number of binding points have a major influence on the mechanical properties of the electrospun mat [17]. The PC type collector operated either in the static or dynamic mode yielded an electrospun mat with the largest number of binding points. Except for collector designs SS and SL, all other types of collector showed a decrease in the number of binding points in the electrospun mat produced in the dynamic mode of operation compared to the static mode of operation. Similarly the mean pore size of the electrospun mat produced by using different collectors when operated in the dynamic mode had a larger mean pore size than the one produced in the static mode of operation of the collector plates. (*Table 2*). The observed variation in the average diameter, number of binding points and mean pore size of mats produced by different collector plates operated in the static or dynamic mode will be reflected in their properties.

Figure 5. *SEM images of the electrospun mat produced using different collectors operated in the static mode: a) H, b) C, c) RS, d) RL, e) SS, f) SL, g) PC.*
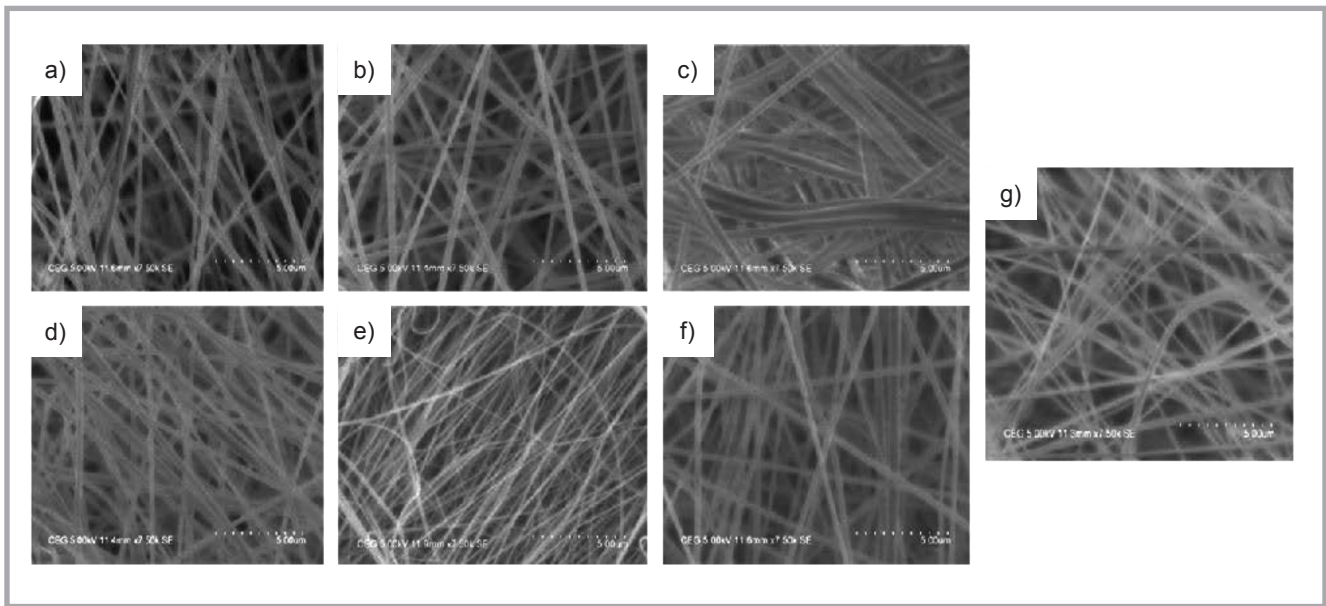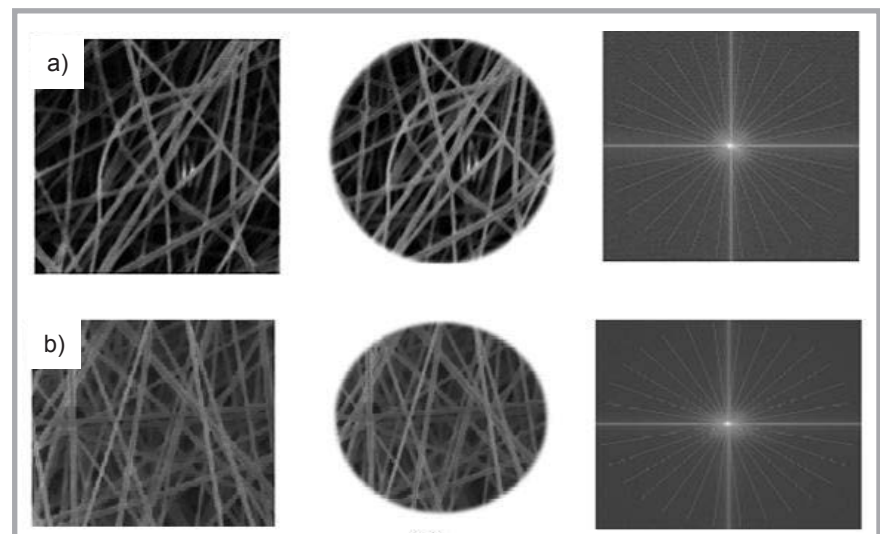
***Figure 6.** SEM images of the electrospun mat produced using different collectors operated in the dynamic mode: a) H, b) C, c) RS, d) RL, e) SS, f) SL, g) PC.*

The FFT method was used to evaluate the relative fiber alignment in the electrospun mat shown in ***Figure 7***.

A comparison of the gray scale intensity of SEM images of electrospun mats produced using different collectors showed that the alignment of fibres along 0/180° directions was the highest, followed by 90°/270° directions, irrespective of the template design and mode of operation of the collector plate (***Figure 8***). The static mode of operation yielded less variation in gray scale intensity for the SEM images of electrospun mats produced using RL, SS, SL and PC collectors. Whereas the dynamic mode of operation yielded less variation in the gray scale intensity of SEM images of the electrospun mat produced using H, C and RS collectors compared to the static mode of operation (***Table 3***). At the onset of the electrospinning process, fibres were deposited at locations which were favourably conductive. Once the possibilities of the conductive path in that region get reduced due to fibre deposition, it would start depositing on other areas. But in the case of the dynamic mode of operation of the collectors, fibre deposition would be based on the conductive path as well as due to the air flow interaction. This might be the reason for the change observed in the percentage of fibre alignment at specific angles when a particular collector is operated in the static and dynamic mode of operation. Among all the collectors, the RS template yielded less variation in the gray scale intensity of the SEM image of

the electrospun mat produced by both the static and dynamic modes of operation (***Table 3***).
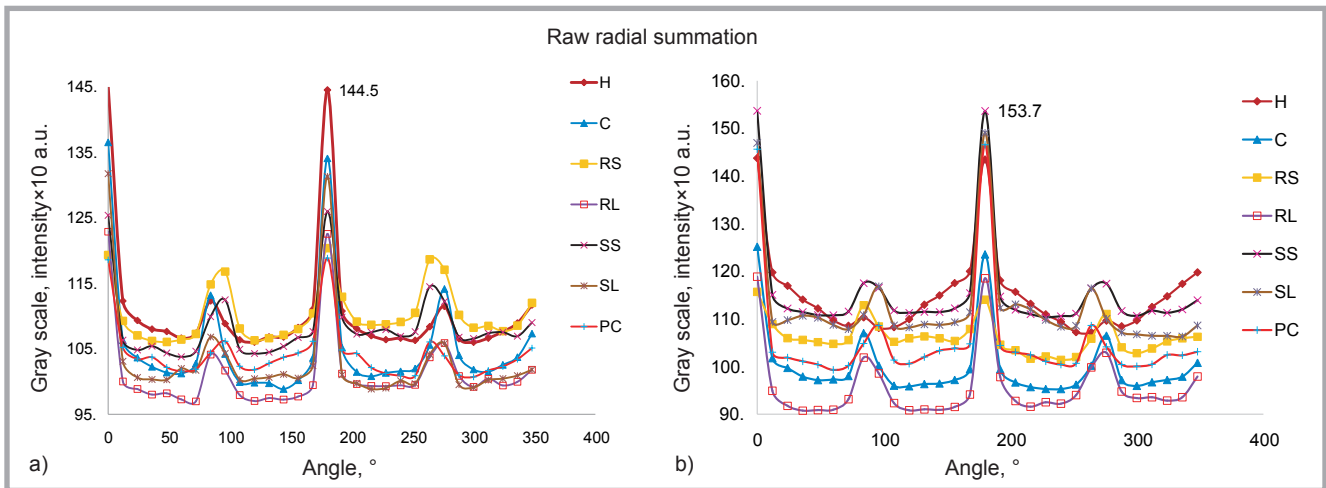
An electrospun mat with uniform thickness is desirable to obtain uniform properties. A graph of the thickness of the


***Figure 7.** FFT analysis of an electrospun mat produced using a collector of type C operated in the a) static and b) dynamic modes (left – SEM image of scaffold, middle – SEM image after processing and right – 2D FFT analysis and raw radial summation).*

***Table 2.** Analysis of SEM images of electrospun mat produced using different collectors operated in static and dynamic conditions.*

Collectors	Average diameter, nm (based on SEM images)		No.of binding points (based on SEM images)		Mean pore size, µm (capillary flow porometer)	
	Static	Dynamic	Static	Dynamic	Static	Dynamic
H	165	254	144	96	0.56	1.08
C	286	253	126	101	0.63	0.85
RS	255	426	134	86	0.46	1.07
RL	273	259	135	100	1.85	0.91
SS	253	109	106	114	0.84	0.73
SL	222	304	89	97	0.74	1.6
PC	230	225	177	121	0.94	1

Figure 8. *FFT analysis of mat collected using different collectors in the a) static and b) dynamic modes of operation.*
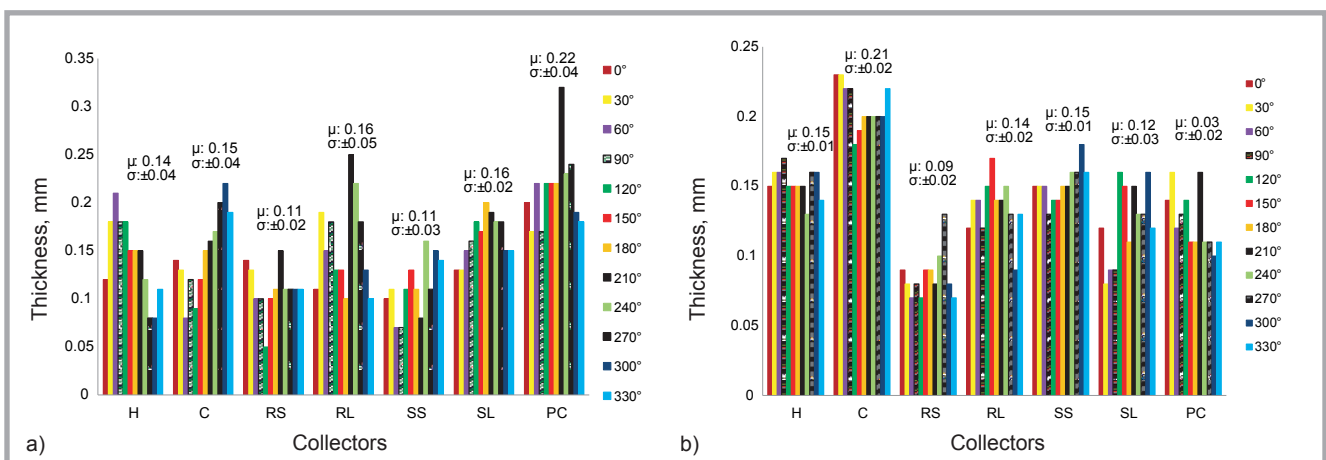
Figure 9. *Thickness of electrospun mat produced using collectors operated in a) static and b) dynamic conditions: (μ – average of thickness measurement at different angles and σ – standard deviation).*

mat at different angular sections of the electrospun mat produced using various collectors is shown in **Figure 9**. While comparing the thickness of electrospun mats obtained from different collectors in a static condition, the thickness was nearly uniform in the electrospun mat produced using collectors of template designs RS and SL.

Among the collectors operating in the static mode, template design PC yielded an electrospun mat with the highest

thickness, and in the case of dynamic operated collectors, it was the electrospun mat produced using collector template C. However the electrospun mat produced using the RS template collector had the advantage of the lowest inhomogeneity in terms of fibre orientation, but has the lowest thickness, no matter if the collector was stationary or rotated. If the uniform thickness is desirable for a particular application, then the dynamic mode of operation of H and SS template collectors can be the best choice.

Properties of the electrospun mat

The pore size and its distribution of the electrospun mat have a significant role in applications like filtration and for scaffolds used in tissue engineering. The pore size of the electrospun mat which was produced using different collectors has a distribution in the range of 0.46-1.85 μm (*Table 2*). The electrospun mat produced using rotating collectors showed a narrower distribution of pore size (0.7-1.2 μm) than that produced using a static collector (0.7-3.3 μm). *Figure 10* shows the distribution of the pore size of the electrospun mat produced using a C type collector, as an example.

Except for RL and SS type collectors, the mean pore size of electrospun mats produced in the dynamic mode of operation of the collectors was higher than for the electrospun mats produced in the static mode of operation. If the least porosity of the electrospun mat is desired for applicaton as film, membrane, etc,
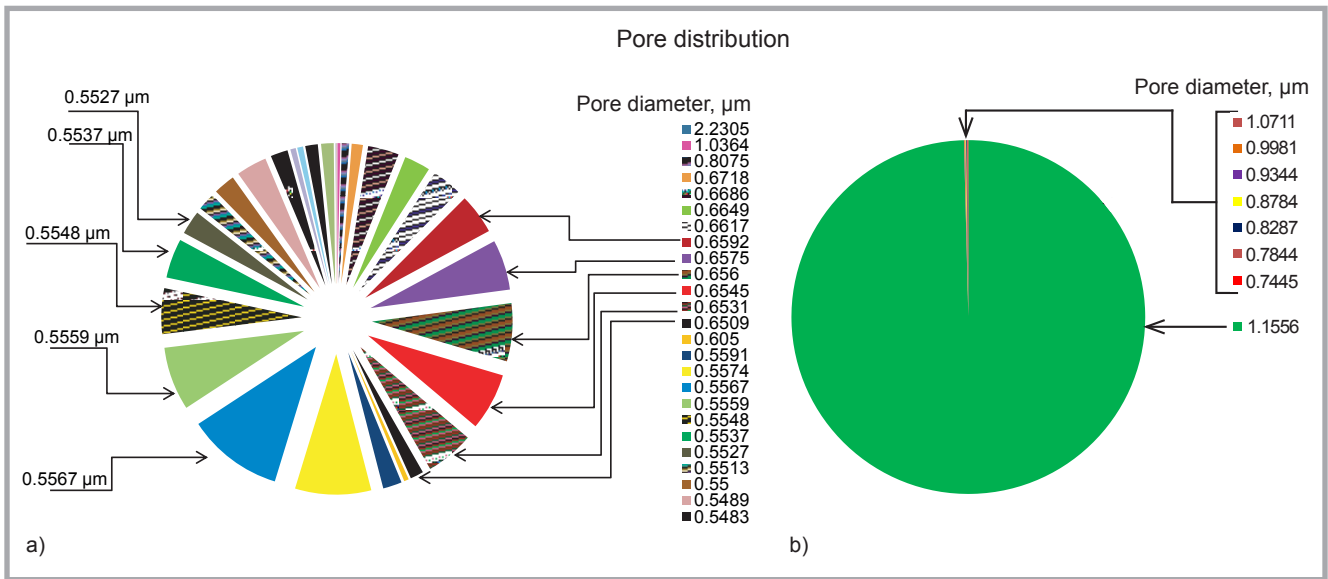
Table 3. *Comparison of Gray scale intensity of 2D FFT SEM images of electrospun mat produced using different collectors operated in static and dynamic conditions.*

	H	C	RS	RL	SS	SL	PC
Static mode of operation							
AVG, μ	110672	105368	110351	101242	108492	103279	104195
STDEV, σ	9501	8859	4221	6217	5317	7915	4284
Dynamic mode of operation							
AVG, μ	114822	100010	106144	95691	115403	112272	105384
STDEV, σ	8782	7219	3477	7071	10627	10050	11302

Figure 10. *Pore size distribution of electrospun mat produced using a C type collector operated in the (a) static mode and (b) dynamic mode.*
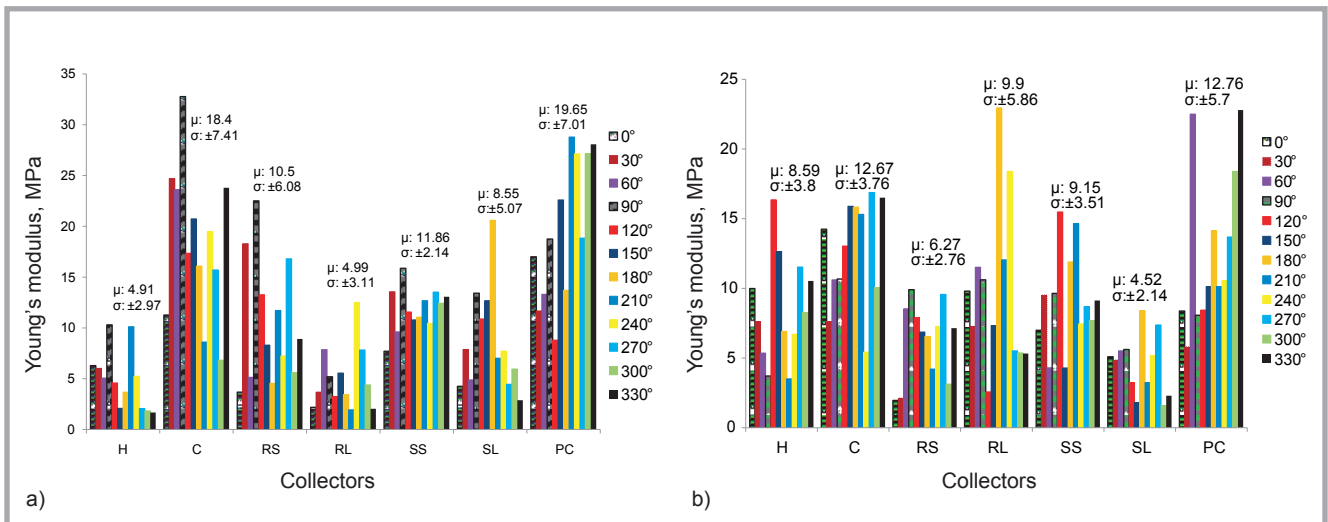

Figure 11. *Young's modulus of an electrospun mat produced using different collectors in the (a) static and (b) dynamic mode (μ – average and σ – standard deviation).*
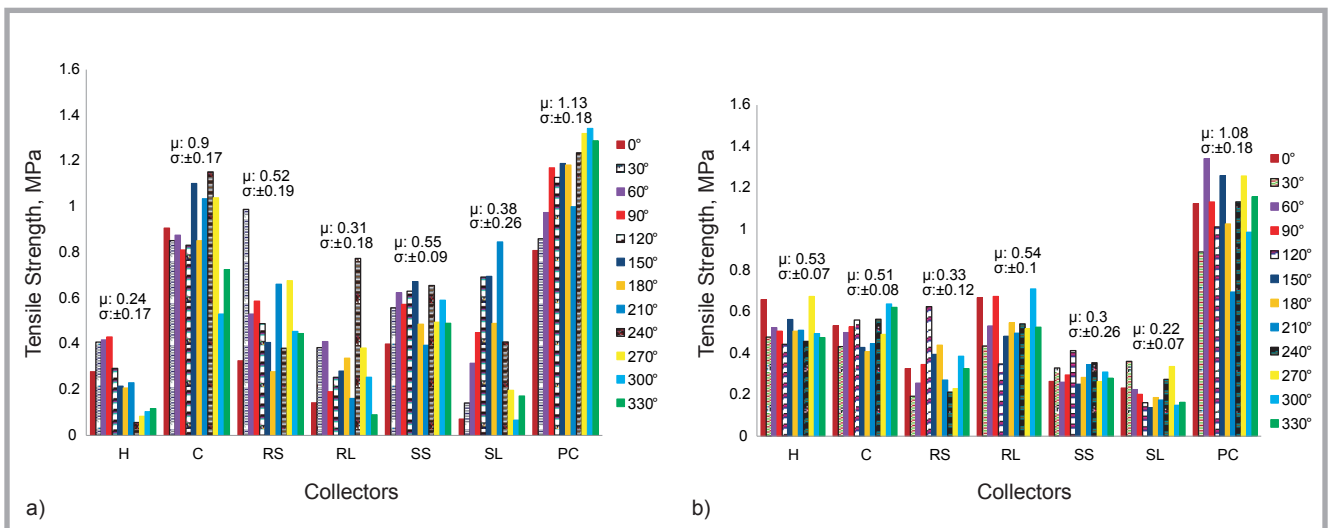

Figure 12. *Tensile strength of an electrospun mat produced using different collectors operated in the (a) static and (b) dynamic mode.*

Table 4. *Decreasing order listing of different collectors operated in static mode for the various properties of electrospun mat.* **Note:** *Average fibre diameter, binding points and porosity are not taken at different angular sections, rather taken randomly and average value is tabulated.*

Surface area of collector plate, m²	Average fiber diameter, nm	No. of binding points	Mean pore size, μm	Thickness, mm			Ultimate tensile strength, MPa			Deflection, mm
					μ	σ		μ	σ	
PC 0.018	C 286	PC 177	RL 1.85	PC	0.22	±0.04	PC	1.13	±0.18	PC 1.3
RS 0.013	RL 278	H 144	PC 0.94	RL	0.16	±0.05	C	0.9	±0.17	RS 2
C 0.010	RS 252	RL 135	SS 0.84	SL	0.16	±0.02	SS	0.55	±0.09	SS 2.1
H 0.008	SS 253	RS 134	SL 0.74	C	0.15	±0.04	RS	0.52	±0.19	C 2.1
SS 0.007	PC 230	C 126	C 0.63	H	0.14	±0.04	SL	0.38	±0.26	H 2.3
RL 0.003	SL 222	SS 106	H 0.56	RS	0.11	±0.02	RL	0.31	±0.18	SL 2.4
SL 0.002	H 165	SL 89	RS 0.46	SS	0.11	±0.03	H	0.24	±0.17	RL 2.8

a stationary RS collector can be the best choice. If the highest porosity is desirable, as in the case of scaffold application, a stationary RL collector can be the best choice.

The variations in the thickness of mat, the orientation and diameter of fibre as well as the pore size would surely influence the mechanical property. Young's modulus and ultimate tensile strength of mat are shown in **Figures 11** and **12** respectively.

Similar to the observations made in the thickness analysis, the dynamic mode of operation of the collectors lessens the variation in Young's modulus for all types of collectors except for the H, RL and SS collectors. The PC type collector demonstrated the highest Young's modulus and moderate variation among dynamically operated collectors, whereas this was the case for the mat produced using a type C collector among the static operated collectors. The collectors of template design H and RL when operated in the dynamic mode yielded a mat with a higher mean Young's modulus than in the static mode.

On analysis of the ultimate tensile strength of the electrospun mat, that produced by collector PC gave high strength in both the static and dynamic modes of operations. For applications which require strength as well as less variation among different sections of the mat, the dynamic operation of collectors H and C are suitable.

In order to compare the overall properties of the electrospun mat produced using collectors operated in the static mode, **Table 4** lists collectors in decreasing order of different features or properties. A mat produced by a PC collector showed a maximum tensile strength of 1.13 MPa and maximum thickness of 0.22 mm. The possible areas of application could be films, membranes and scaffolds for muscle/nerve regeneration. The probable reason for better properties may be due to the larger surface area of the collector. If the desired property is the porosity of the electrospun mat and not the strength, an RL collector can be suitable and applications can be 3D scaffolds for tissue engineering. The type C collector produced an electrospun mat with a tensile strength of 0.9 MPa and fiber diameter of 286 nm, which is desirable for application as a membrane and filtration.

Table 5. *Decreasing order listing of different collectors operated in dynamic mode for the various properties of electrospun mat.* **Note:** *Average fibre diameter, binding points and porosity are not taken at different angular sections, rather taken randomly and average value is tabulated.*

Surface area, m²	% Porosity of collector	Fiber diameter, nm	No. of binding points	Mean pore size, μm	Thickness, mm			Ultimate tensile strength, MPa			Deflection, mm
						μ	σ		μ	σ	
PC 0.017	SS 89	RS 426	PC 121	SL 1.6	C	0.21	±0.02	PC	1.08	±0.18	PC 1
RS 0.012	RL 84	SL 304	SS 114	H 1.09	H	0.15	±0.01	RL	0.54	±0.1	C 1.1
C 0.01	SS 58	RL 259	C 101	RS 1.07	SS	0.15	±0.01	H	0.53	±0.07	RS 1.5
H 0.008	H 54	H 254	RL 100	PC 1.01	RL	0.14	±0.02	C	0.51	±0.08	RL 1.7
SS 0.007	C 42	C 253	SL 97	RL 0.91	PC	0.13	±0.02	RS	0.33	±0.12	SS 2
RL 0.002	RS 28	PC 225	H 96	C 0.85	SL	0.12	±0.03	SS	0.3	±0.26	SL 2.1
SL 0.001	PC 0	SS 109	RS 86	SS 0.73	RS	0.09	±0.02	SL	0.22	±0.07	H 2.2

Table 5 lists different collectors operated in the dynamic mode in decreasing order of properties or features of the mat. Interestingly the PC collector produced a mat with the best mechanical properties, but its thickness and porosity were avergae. For applications like scaffolds, the H type collector, which produced an electrospun mat which is thicker and more porous, could be an option. Overall observation showed that the dynamic mode of operation lessens the variation in properties

of the electrospun mat, which is desired when a great number of sections from the whole mat may suffice for an application, for example, wound dressing scaffold.

While comparing the performance of the electrospun mat produced using a specific template design, for example the SS collector, it was observed that the dynamic mode of operation produced a mat with lower porosity and tensile strength than those of the mat produced in the static mode of operation. The drag force due to the interaction of air flow caused by the rotation of the collector and stream of polymer jets was expected to alter the deposition of the electrospun mat. The amount of air flow depends on the shape and size of holes on the collector at the onset of the collection of the electrospun mat. After sometime, the flow of air is reduced due to the partially deposited electrospun mat, which would determine the porosity of subsequent deposited electrospun fibres.

The mechanical properties of the electrospun mat produced using different collectors operated in the static mode were governed by the surface area of the collector, number of binding points, fibre diameter, pore size and thickness of the mat. Among all factors, the thickness and pore size of the electrospun mat are the most influential. In the case of the dynamic mode of operation of the collectors, additionally the drag force due to air flow along the rotating collector on the approaching stream of polymer jets would have also influenced the properties of theelectrospun mat. Thus it was difficult to ascertain the reasons for the change in the trend of properties due to the dynamic mode of operation of collectors of seven different template designs with current experimental data and analysis.

■ Conclusions

The design of the template of the collectors influenced the properties of the electrospun mat produced. The dynamic mode of operation of most types of collectors yielded an electrospun mat with a low mean value of properties compared to that of the static mode. This study reveals that different collectors of the electrospinning process when operated in the dynamic mode lessened the inhomogeneity in properties among the different angular sections of the mat compared to the mat produced by using the static mode of operation of the collectors. Based on the desired combination of properties such as Young's modulus, ultimate tensile strength, pore size and thickness, a collector and its mode of operations can be selected.

❑

References

1. Sahay R, Thavasi V and Ramakrishna S. *J Nanomater* DOI:10.1155/2011/317673.
2. Huang Z, Zhang Y Z, Ktaki M and Ramakrishna S. *Compo Sci Technol* 2003; 63: 2223-2253.
3. Yiquan W, Zexuan D, Scott W and Robert L C. *Polymer* 2010; 51: 3244-3248.
4. Haiyan L, Yachen X, He X and Jiang C. *J. Mater. Chem. B* 2014; 2: 5492-5510.
5. Bin S, Xue-Jun J, Shuchao Z, Jun-Cheng Z, Yi-Feng L, Qin-Zhong Y and Yun-Ze L. *J. Mater. Chem. B* 2015; 3: 5389-5410.
6. Da Y, John J, Xiaoyan Y, Xinhua X, Jing S, James C-M L, Guiqiu M, Qingsong Y. *J. Med. Biol. Eng.* 2013; 33: 171-178.
7. Chieh C, Kevin L and Liwei L. *Appl. Phys. Lett.* 2008; 93: 123111-(1-3).
8. Shifang Z, Qihui Z, Yun-Ze L, Guang-Hui S and Yanzhong Z. *Nanoscale* 2013; 5: 4993-5000.
9. Daming Z and Jiang C. *Adv. Mater.* 2007; 19: 3664-3667.
10. Vaquette C and Cooper-White J J. *Acta Biomater* 2011; 7: 2544-2557.
11. Yazhou W, Guixue W, Liang C, Hao L, Tieying Y, Bochu W, James C-M L and Qingsong Y. *Biofabrication* DOI: 10.1088/1758-5082/1/1/015001.
12. Matthew R M, Jingwei X, Zack R and Younan X. *US Patent* US20130197663A1, 2013.
13. Nuno M N, Rui C, Adriano P, Jose C, Francisco M, Rui L R. *Int. J. Nanomedicine* 2007; 2: 433-448.
14. Iman H, Mahmoud M M and Ghader F. *Chem Phys Lett* 2013; 590: 231-234.
15. Milasius R and Malasauskiene J. *Autex Res J* 2014; 4: 233-238.
16. Chantal E A, Shekhar Jha B, Hannah M, James R B, Gary L B, Scott C. H and David G S. *J. Biomater. Sci. Polym Edn* 2008; 19: 603-621.
17. Xiaofan W, Zhenhai X, Shing-Chung W and Avinash B. *Int J Exp and Comput Biomech* 2009; 1: 45-57.